

# A CAE modeling approach for the analysis of vibro-acoustic systems with distributed ASAC control

Leopoldo P.R. de Oliveira\*, Arnaud Deraemaeker °, Jan Mohring<sup>†</sup>, Herman Van der Auweraert<sup>†</sup>, Paul Sas\*, Wim Desmet\*

\* Katholieke Universiteit Leuven - Department of Mechanical Engineering  
Celestijnenlaan 300B, B-3001, Leuven – Belgium

° Université Libre de Bruxelles - Active Structures Laboratory  
Avenue F.D. Roosevelt, 50 B-1050 Brussels – Belgium

<sup>†</sup> Fraunhofer-Institut für Techno- und Wirtschaftsmathematik  
Fraunhofer-Platz 1 67663 Kaiserslautern – Germany

<sup>†</sup> LMS International  
Interleuvenlaan 68, B-3001, Leuven – Belgium  
email: [leopoldo.deoliveira@mech.kuleuven.be](mailto:leopoldo.deoliveira@mech.kuleuven.be)

## Abstract

The aim of this paper is to present a CAE methodology for simulating coupled vibro-acoustic systems and include these models into a closed loop control simulation. This tool provides a reliable simulation procedure that takes into account the vibro-acoustic phenomena as well as the control system since sensors/actuators models and the control algorithms can be included. The focus of the present paper is on the active structural-acoustic control, using piezoelectric patches as sensors and actuators. An initial structural uncoupled finite element model is modified to account for the placement of piezo-patches. The modified structural modal base is then used together with an uncoupled acoustic modal base to derive the fully coupled vibro-acoustic finite element model, which is reduced and formulated as a state-space model. The electro-mechanical coupling between the structure and the sensor/actuator pair is calculated and included in the state-space model. Eventually, a feedback controller is implemented. This smart-structure modeling approach is illustrated for the case of the active reduction of the sound transmission of a firewall between the engine and the passenger compartments of a concrete car-like demonstrator.

## 1 Introduction

The demands for improvement in sound quality and reduction of noise generated by machines and means of transportation are steadily increasing. For the transportation industry, the sound generated by their products is becoming more a design issue rather than a threshold limit avoided after conservative design measures. On the other hand the amount of space and weight penalty that passenger vehicles can handle is limited. A promising approach to cope with this challenge is the use of active control, either active noise control (ANC) or active structural-acoustic control (ASAC).

During the design stages, simulation plays an important role in predicting the performance and feasibility of active control solutions. The use of proper simulation techniques can result in cost and time reduction in the development stages, since it enables the engineer to compare different strategies, sensor and actuator configurations and control algorithms. However, to bring the application of active solutions to the product development phase, the simulation techniques involved must be based on typical simulation tools such as finite element (FE) or boundary element (BE) methods.

In a vehicle, the low-frequency noise is usually transmitted into the vehicle's cabin through structural paths, which raises the necessity of dealing with vibro-acoustic models. For ASAC simulation, these models have to integrate not only structural and acoustical components, but also the control sensors, actuators and the controller logic. The importance of including detailed information about the controller is

critical for an accurate assessment of its actual performance, since sensor and actuator dynamics can present frequency, phase and amplitude limitations.

This paper describes a methodology for ASAC simulation based on fully coupled vibro-acoustic systems including piezoelectric sensor/actuators models. The system under study is a simplified rigid car cavity with engine and passenger compartments, separated by a flexible firewall. The active control system consists of a collocated piezo-electric sensor/actuator pair (SAP) placed on the firewall and connected in a feedback loop. The modeling procedure allows the choice of the ideal feedback gain, in order to achieve the maximum reduction on the sound pressure level at the driver's ear, due to a noise disturbance in the engine compartment.

## 2 Smart structure modeling approach and validation case

The Sound Brick set-up at LMS International has been selected to demonstrate the modeling procedures described in this section. It consists of a simplified car cavity with concrete walls to provide well-defined acoustic boundary conditions, thus avoiding uncertainties during the vibro-acoustic modeling phase.

A previous version of the setup is shown in Fig.1a. The current configuration has a flexible firewall and a rigid engine compartment (EC) as in Fig.1b. A sound source placed in the EC acts as a primary disturbance source. The firewall is assembled between the EC and the passenger cavity (PC) which allows a set of structural sensors and actuators to realize the control signals for increasing the firewall transmission loss between the cavities. The PC main dimensions are about 3400 x 1560 x 1270mm; for the EC, 900 x 1100 x 750mm and the firewall 920 x 545 x 1.5mm. The firewall has clamped boundaries.

Two collocated piezo-patches, 46 x 54.5 x 0.3mm, relative permittivity  $\epsilon_r = 1800$  and piezoelectric constants  $d_{31} = d_{32} = -190 \cdot 10^{-12} \text{m/V}$ , work as a collocated SAP. The actuator patch receives a voltage proportional to the time derivative of the charge generated by the sensor patch. The feedback gain is chosen based on the achievable reduction on the noise evaluated at the driver's ear.

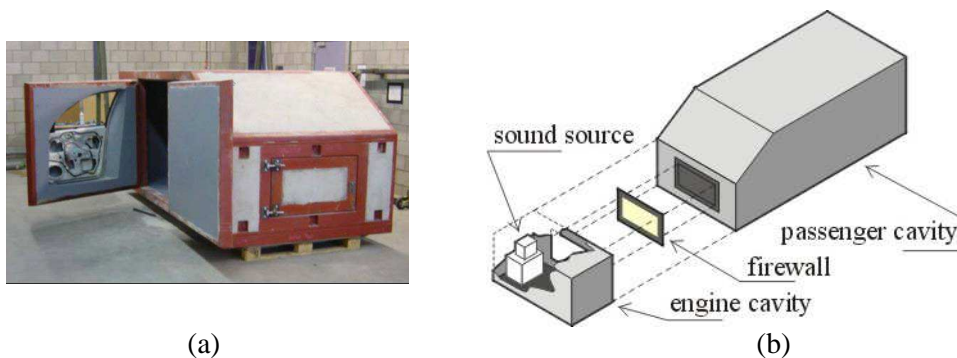


**Figure 1 – System under investigation (a) photo (b) schematic view**

In view of having a smart structure modeling approach for vibro-acoustic systems, a coupled vibro-acoustic FE/FE modeling approach is adopted. In this way, the whole system is subject to acoustic excitation from both cavities which allows the use of the primary source in the EC, but would be suitable also for the use of secondary sources in either of the cavities. It is also possible to use structural excitation, as disturbance and/or control actuation, as well as acoustic (pressure) and/or structural (displacement) sensors.

Another advantage of using a fully coupled vibro-acoustic approach is the accuracy of the estimated performance in the ASAC simulation, as an uncoupled analysis can overestimate the controller efficiency [1]. It is also required that the modeling approach fits into an optimization loop [16], as the design of an ASAC system usually requires the tuning of some controller parameters (SAP position, gains, etc.).

However, vibro-acoustic FE/FE models can easily reach hundreds of thousands of degrees of freedom, thus resulting in large computation effort and CPU time. If such models are part of an optimization loop, where new vibro-acoustic transfer functions and/or forced responses are needed for every iteration, the size of such models are crucial for the optimization feasibility.

The electro-vibro-acoustic system of equation in the frequency domain, in terms of the structural displacements  $\mathbf{u}$ , acoustic pressure  $\mathbf{p}$  and voltage  $\mathbf{v}$ , can be written as:

$$\left( \begin{bmatrix} \mathbf{K}_s & \mathbf{K}_c & \mathbf{K}_{se} \\ \mathbf{0} & \mathbf{K}_a & \mathbf{0} \\ \mathbf{K}_{es} & \mathbf{0} & \mathbf{K}_e \end{bmatrix} + j\omega \begin{bmatrix} \mathbf{C}_s & \mathbf{0} & \mathbf{0} \\ \mathbf{0} & \mathbf{C}_a & \mathbf{0} \\ \mathbf{0} & \mathbf{0} & \mathbf{0} \end{bmatrix} - \omega^2 \begin{bmatrix} \mathbf{M}_s & \mathbf{0} & \mathbf{0} \\ \mathbf{M}_c & \mathbf{M}_a & \mathbf{0} \\ \mathbf{0} & \mathbf{0} & \mathbf{0} \end{bmatrix} \right) \begin{Bmatrix} \mathbf{u}(\omega) \\ \mathbf{p}(\omega) \\ \mathbf{v}(\omega) \end{Bmatrix} = \begin{Bmatrix} \mathbf{f}_s(\omega) \\ \mathbf{f}_a(\omega) \\ \mathbf{Q}(\omega) \end{Bmatrix} \quad (1)$$

where  $\mathbf{K}$ ,  $\mathbf{C}$  and  $\mathbf{M}$  are, respectively, the stiffness, damping and mass matrices,  $\mathbf{f}$  is the load vector,  $\mathbf{Q}$  is the charge on the piezo-patch, the index  $s$  refers to structural components,  $a$  to acoustic components,  $c$  to vibro-acoustic coupling,  $e$  to electrical components and  $se$  and  $es$  to electro-mechanical coupling.

As it can be seen from the stiffness matrix in Eq.(1), there is no coupling between the acoustic and electrical components, which allows a stepwise modeling procedure, where the mechanical and electrical contributions of the piezo-patches are taken separately.

The full modeling procedure is illustrated in Fig.2. The structural FE model is modified to account for the placement of the piezo-patches, which is done by modifying the mass and stiffness properties of the elements corresponding to the sensor and actuator positions. A modal base that already contains the mechanical contribution of the piezo-patches can then be obtained. This modal base is used together with the uncoupled acoustic modal base of both cavities to derive the vibro-acoustic FE model from which a coupled vibro-acoustic modal base is extracted. Using the electro-mechanical formulation of the piezoelectric elements in terms of the modal structural displacements, it is possible to include the electrical degrees of freedom (DoFs) in the current modal formulation. The fully coupled electro-vibro-acoustic modal model, written through a state-space formulation, allows the implementation of control strategies involving the piezo-patches and the vibro-acoustic system.

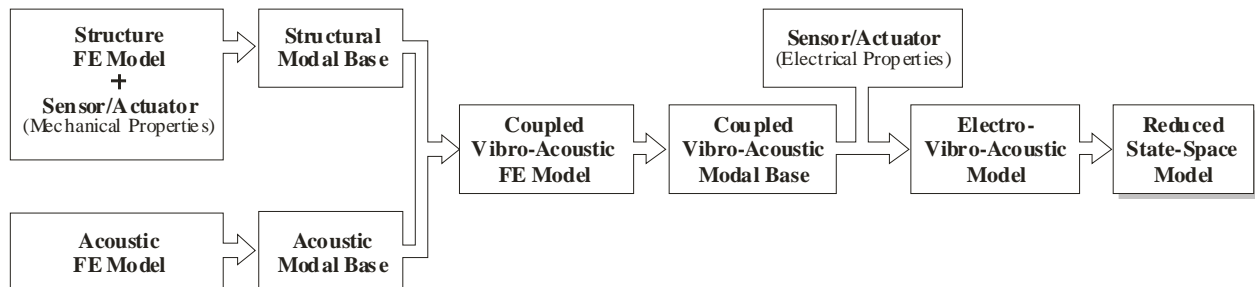


Figure 2 – Modeling procedure scheme

Table 1 shows the physical properties of each component.

Table 1 – Components physical properties

	density [g/m <sup>3</sup> ]	elasticity modulus [Pa]	speed of sound [m/s]
firewall	7800	2.33 e <sup>11</sup>	-
piezo-patches	7800	6.60 e <sup>10</sup>	-
acoustic cavities	1.163	-	349.6

### 3 Vibro-acoustic modeling

A first step in the modeling of the vibro-acoustic behavior of a structure with finite elements is the definition of appropriate meshes for the acoustic and structural components. Since acoustic wavelengths are usually longer than structural ones, optimized acoustic meshes can be much coarser than structural meshes. However, if the meshes are compatible, some intermediate numerical steps [2] can be neglected resulting in a simplified procedure. Therefore a trade-off choice for the size of structural and acoustic FE meshes was taken, allowing them to have coinciding nodes on the interface. Using Patran, the size of the structural elements was chosen as large as possible so that the shortest wavelength could be represented by at least 8 linear elements. In the frequency range of interest (0 to 200Hz), the shortest structural wavelength occurs at 192Hz as depicted in Table 2 and Fig. 3. The acoustic mesh size was created (also in Patran) based on the structural one and has a minimum of 10 linear elements per wavelength up to 308Hz.

Table 2 shows the resonance frequencies for the coupled vibro-acoustic model and the uncoupled structural and acoustical components, as calculated by Sysnoise (except for the structural component, for which Nastran was used). It also shows the mode shapes in terms of the number of wavelengths in the  $x$ ,  $y$  and  $z$  directions for the uncoupled modes.

**Table 2 – Resonance frequencies for coupled and uncoupled systems**

coupled vibro-acoustic modes		uncoupled structural modes		uncoupled acoustic modes	
mode #	freq. [Hz]	freq. [Hz]	half-wavelengths (y, z)	freq. [Hz]	wavelengths (x, y, z)
1	0			0	EC - (0,0,0)
2	0			0	PC - (0,0,0)
3	35.12	33.90	(1,1)		
4	47.85	47.96	(2,1)		
5	53.80			53.43	PC - (1,0,0)
6	72.76	72.65	(3,1)		
7	85.75	85.77	(1,2)		
8	98.32	98.32	(2,2)		
9	104.7			104.6	PC - (2,0,0)
10	107.3	107.5	(4,1)		
11	112.2			112.1	PC - (0,1,0)
12	119.9	120.0	(3,2)		
13	124.2			124.2	PC - (1,1,0)
14	139.5			139.5	PC - (0,0,1)
15	149.5			149.7	PC - (3,0,0)
16	151.2	151.2	(4,2)		
17	152.3	152.2	(5,1)		
18	153.3			153.3	PC - (3,1,0)
19	160.3			160.4	PC - (4,0,0)
20	161.6			161.5	EC - (0,1,0)
21	164.3	164.2	(1,3)		
22	177.0	176.7	(2,3)		
23	179.0			179.0	PC - (0,1,1)
24	184.7			183.7	EC - (1,0,0)
25	185.6			185.6	PC - (2,0,1)**
26	192.4	192.4	(5,2)*		
27	196.9	196.8	(3,3)		

\* mode depicted in Fig. 3

\*\* mode depicted in Fig. 4

EC = Engine Compartment

PC = Passenger Compartment

The structural mesh (Fig.3a) has 200 4-noded shell elements. The steel firewall of 1.5mm thickness presents 13 modes from 0 to 200Hz. It is important to notice that the inclusion of the mechanical properties of sensors and actuators takes place in this step, by including the mechanical behavior of the piezo-patches as extra layers in the finite element shell model. In this way, the structural modal base already includes the mechanical influence of the sensors and actuators.

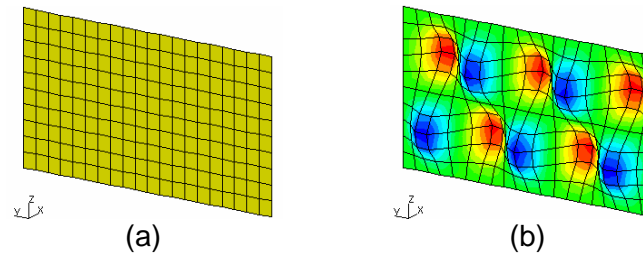


**Figure 3 – Firewall: (a) FE mesh and (b) uncoupled mode (5,2)**

The element type chosen for the acoustic mesh is the 8-noded brick. This element was preferred over the tetrahedral element because of the smaller number of elements needed and the higher accuracy in post-processing secondary quantities (velocity and sound intensity) [3]. The size of the structural elements and the maximum frequency of interest (200Hz for this study case) were taken into account to define the acoustic mesh discretization, so that the acoustic model could have coinciding nodes with the structural mesh while having a minimum number of elements. The resulting mesh with 25000 elements and the highest mode shape at 185.6Hz are depicted in Fig.4. With respect to the element size, this acoustic model is valid up to 308Hz, considering a minimum of 10 linear elements per wavelength.

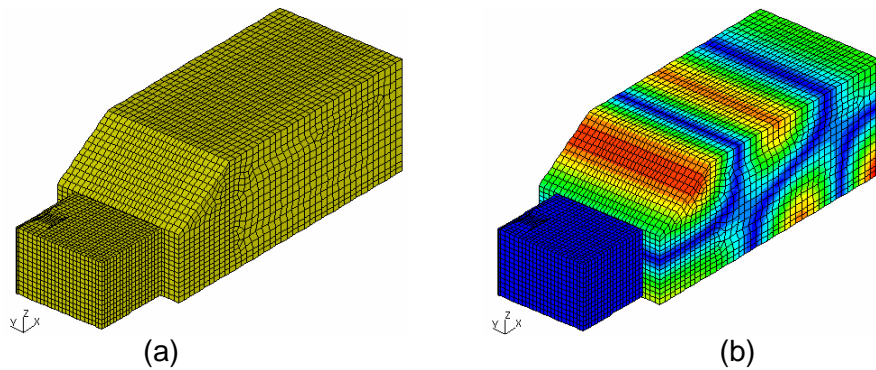


**Figure 4 – Cavities: (a) FE mesh and (b) uncoupled mode at 185Hz**

The structural and acoustic models are fully-coupled in this FE/FE approach. The effect of the fluid on the structure dynamics can be considered as a pressure load on the wetted surface, turning the structural differential equation into the form of Eq.(2).

$$\left( \mathbf{K}_s + j\omega \mathbf{C}_s - \omega^2 \mathbf{M}_s \right) \mathbf{u}(\omega) + \mathbf{K}_c \mathbf{p}(\omega) = \mathbf{f}_s(\omega) \quad (2)$$

where  $\mathbf{K}_s$ ,  $\mathbf{C}_s$  and  $\mathbf{M}_s$  are, respectively, the stiffness, damping and mass matrices of the structural component modified by the presence of the piezo-patches,  $\mathbf{K}_c$  is the coupling matrix,  $\mathbf{u}$  is the vector of structural displacements,  $\mathbf{p}$  is the vector of acoustic pressures and  $\mathbf{f}_s$  is the structural load vector.

In a similar way, the structural vibrations provide an acoustic velocity input and therefore must be taken into account in the acoustic model as:

$$\left( \mathbf{K}_a + j\omega \mathbf{C}_a - \omega^2 \mathbf{M}_a \right) \mathbf{p}(\omega) - \omega^2 \mathbf{M}_c \mathbf{u}(\omega) = \mathbf{f}_a(\omega) \quad (3)$$

where  $\mathbf{K}_a$ ,  $\mathbf{C}_a$  and  $\mathbf{M}_a$  are the acoustical stiffness, damping and mass matrices,  $\mathbf{M}_c$  is the coupling matrix, and  $\mathbf{f}_a$  is the acoustic load vector. For the sake of brevity, any frequency dependent function ' $h(\omega)$ ' is represented just as ' $h$ ' hereafter.

Using the relation  $\mathbf{M}_c = -\rho_0 \mathbf{K}_c^T$  [4], the combined system of equations, known as the Eulerian FE/FE model, yields:

$$\left( \begin{bmatrix} \mathbf{K}_s & \mathbf{K}_c \\ \mathbf{0} & \mathbf{K}_a \end{bmatrix} + j\omega \begin{bmatrix} \mathbf{C}_s & \mathbf{0} \\ \mathbf{0} & \mathbf{C}_a \end{bmatrix} - \omega^2 \begin{bmatrix} \mathbf{M}_s & \mathbf{0} \\ -\rho_0 \mathbf{K}_c^T & \mathbf{M}_a \end{bmatrix} \right) \begin{Bmatrix} \mathbf{u} \\ \mathbf{p} \end{Bmatrix} = \begin{Bmatrix} \mathbf{f}_s \\ \mathbf{f}_a \end{Bmatrix} \quad (4)$$

Based on Eq.(4) it is clear that the resulting vibro-acoustic system is coupled, though it is no longer symmetric. As a consequence of such non-symmetric nature, the solution of the associated eigenproblem is computationally more demanding and results in different left and right eigenvectors.

A common practice in solving such vibro-acoustic problems is the use of component mode synthesis (CMS) [4]. It consists of expanding the structural DoFs in terms of a set of  $N_s$  uncoupled structural modes  $\Phi_s$  (without any acoustic pressure load along the coupling interface), as well as the acoustic DoFs in terms of a set of  $N_a$  uncoupled acoustic modes  $\Phi_a$  (acoustic boundaries considered perfectly rigid). The structural and acoustic expansions become respectively,

$$\mathbf{u} = \sum_{r=1}^{N_s} q_{s_r} \{\Phi_s\}_r = \Phi_s \mathbf{q}_s \quad (5)$$

$$\mathbf{p} = \sum_{r=1}^{N_a} q_{a_r} \{\Phi_a\}_r = \Phi_a \mathbf{q}_a \quad (6)$$

Substituting the component mode expansions in Eqs.(5) and (6) into Eq.(4) and pre-multiplying the structural and acoustical parts of the resulting matrix equation, respectively with the transpose of the structural and acoustic modal vectors yields the modal representation:

$$\left( \begin{bmatrix} \tilde{\mathbf{K}}_s & \Phi_s^T \mathbf{K}_c \Phi_a \\ \mathbf{0} & \tilde{\mathbf{K}}_a \end{bmatrix} + j\omega \begin{bmatrix} \tilde{\mathbf{C}}_s & \mathbf{0} \\ \mathbf{0} & \tilde{\mathbf{C}}_a \end{bmatrix} - \omega^2 \begin{bmatrix} \tilde{\mathbf{M}}_s & \mathbf{0} \\ -\rho_0 \Phi_s \mathbf{K}_c^T \Phi_a^T & \tilde{\mathbf{M}}_a \end{bmatrix} \right) \begin{Bmatrix} \mathbf{q}_s \\ \mathbf{q}_a \end{Bmatrix} = \begin{Bmatrix} \Phi_s^T \mathbf{f}_s \\ \Phi_a^T \mathbf{f}_a \end{Bmatrix} \quad (7)$$

where  $\tilde{\mathbf{K}}$ ,  $\tilde{\mathbf{C}}$  and  $\tilde{\mathbf{M}}$  are the modal stiffness, damping and mass matrices,  $\mathbf{q}$  is the vector of modal amplitudes and the indexes  $s$  and  $a$  denote, respectively, the uncoupled structural and acoustical components.

Regarding that each mode set is normalized with respect to its own uncoupled mass matrix, Eq.(7) can be rewritten as:

$$\left( \begin{bmatrix} \Omega_s^2 & \Phi_s^T \mathbf{K}_c \Phi_a \\ \mathbf{0} & \Omega_a^2 \end{bmatrix} + j\omega \begin{bmatrix} \Gamma_s & \mathbf{0} \\ \mathbf{0} & \Gamma_a \end{bmatrix} - \omega^2 \begin{bmatrix} \mathbf{I}_s & \mathbf{0} \\ -\rho_0 \Phi_s \mathbf{K}_c^T \Phi_a^T & \mathbf{I}_a \end{bmatrix} \right) \begin{Bmatrix} \mathbf{q}_s \\ \mathbf{q}_a \end{Bmatrix} = \begin{Bmatrix} \tilde{\mathbf{F}}_s \\ \tilde{\mathbf{F}}_a \end{Bmatrix} \quad (8)$$

where  $\Omega$  is the diagonal matrix of uncoupled natural frequencies,  $\Gamma$  is the modal damping diagonal matrix and  $\mathbf{I}$  is the identity matrix.

Since this formulation is based on the uncoupled eigenvalue solution of each component, the assembly of the system of equations in (8) is less demanding when compared to the solution of Eq.(4). However, the reduction on the computational effort is rather smaller; beyond the necessity of retaining high-order acoustic modes to achieve the same accuracy as in Eq.(4) [4], the derivation of the state space model still requires the non-symmetric system of equation in (8) to be diagonalized. Nevertheless, the advantage of the CMS is the possibility of using dedicated software to each component.

Using Sysnoise it is possible to calculate the coupled modal base using the uncoupled modal base of each component. When coupling two modal models in Sysnoise, as in Eq.(8), those uncoupled modal vectors are linearly combined to obtain a set of coupled modal vectors for both, acoustic and structural DoFs [5]. These modal vectors can be interpreted as the right eigenvectors from the non-symmetric system of equations on the left-hand side of Eq.(4).

It has been indicated [6] that, particularly for the Eulerian formulation (Eq.4), the left and right eigenvectors, denoted here respectively by  $\Phi_L$  and  $\Phi_R$  can be related as:

$${}_r \Phi_L = \begin{Bmatrix} {}_r \Phi_{Ls} \\ {}_r \Phi_{La} \end{Bmatrix} = \begin{Bmatrix} {}_r \Phi_{Rs} \omega_r^2 \\ {}_r \Phi_{Ra} \end{Bmatrix} \quad (r = 1, 2, \dots, N_s + N_a) \quad (9)$$

where the sub-indexes **s** and **a** denote, respectively, the structural and acoustical components and  $\omega$  is the natural frequency. Using the modal base furnished by Sysnoise and Eq.(9), it is possible to retrieve the left eigenvectors to build the complete modal model, which will be the base for the state space formulation described in more detail in a further section.

## 4 Piezoelectric Actuator and Sensor modeling

The piezo-patches are modeled as multilayer shell elements (Fig.5) which is one of the special elements available in the Samcef FE code. The placement of a sensor and/or actuator is realized by applying the mechanical and electrical properties of the patch to the very external layers of the shell element. Also, an extra DoF is added for each piezoelectric element which will be associated to the voltage applied to an actuator or the charge coming out of a sensor. The equation that governs the dynamics of such an electro-mechanical system is [7]:

$$\left( \begin{bmatrix} \mathbf{K}_s & \mathbf{K}_{se} \\ \mathbf{K}_{es} & \mathbf{K}_e \end{bmatrix} + j\omega \begin{bmatrix} \mathbf{C}_s & \mathbf{0} \\ \mathbf{0} & \mathbf{0} \end{bmatrix} - \omega^2 \begin{bmatrix} \mathbf{M}_s & \mathbf{0} \\ \mathbf{0} & \mathbf{0} \end{bmatrix} \right) \begin{Bmatrix} \mathbf{u} \\ \mathbf{v} \end{Bmatrix} = \begin{Bmatrix} \mathbf{f}_s \\ \mathbf{Q} \end{Bmatrix} \quad (10)$$

The electro-mechanical coupling matrices  $\mathbf{K}_{se}$  and  $\mathbf{K}_{es}$  are mutually transposed, so that the coupled stiffness matrix is symmetric. The vector  $\mathbf{u}$  represents the structural displacements and the load vectors  $\mathbf{f}_s$  is the force input to the structure. Notice that in this set of equations the actual input voltage  $\mathbf{V}$  is on the left-hand side, while the sensed charge  $\mathbf{Q}$  on the patch, is on the right-hand side. As mentioned before, the mechanical contribution of the patches has already been considered during the structural FE modeling, i.e.,  $\mathbf{K}_s$  and  $\mathbf{M}_s$  contain the piezo mass and stiffness contributions.

The strategy is to use the modal expansion given by Eq.(5) for Eq.(10), and pre-multiply the first line by the transposed modal matrix  $\Phi_s$ .

$$\left( \begin{bmatrix} \Phi_s^T \mathbf{K}_s \Phi_s & \Phi_s^T \mathbf{K}_{se} \\ \mathbf{K}_{es} \Phi_s & \mathbf{K}_e \end{bmatrix} + j\omega \begin{bmatrix} \Phi_s^T \mathbf{C}_s \Phi_s & \mathbf{0} \\ \mathbf{0} & \mathbf{0} \end{bmatrix} - \omega^2 \begin{bmatrix} \Phi_s^T \mathbf{M}_s \Phi_s & \mathbf{0} \\ \mathbf{0} & \mathbf{0} \end{bmatrix} \right) \begin{Bmatrix} \mathbf{q}_s \\ \mathbf{v} \end{Bmatrix} = \begin{Bmatrix} \Phi_s^T \mathbf{f}_s \\ \mathbf{Q} \end{Bmatrix} \quad (11)$$

Voltage actuation and charging sensing are considered. Actuation is done by imposing the desired voltage, whereas sensing by imposing the voltage to be zero. In this way, the actuator equation (12) and sensor equation (13) can be extracted from the first and the second lines of Eq.(11) respectively.

$$\Phi_s^T \left( \mathbf{K}_s + j\omega \mathbf{C}_s - \omega^2 \mathbf{M}_s \right) \Phi_s \mathbf{q}_s = \Phi_s^T \mathbf{f}_s - \Phi_s^T \mathbf{K}_{se} \mathbf{v} \quad (12)$$

$$\mathbf{Q} = \mathbf{K}_{es} \Phi_s \mathbf{q}_s \quad (13)$$

Note that the final actuation system (Eq.12) takes the form of a purely structural one with additional loads associated with the applied voltages. Ever since the specific formulation for such elements is available, it is possible to include as many piezo-patches as needed, regarded that an extra DoF is needed for every sensor or actuator.

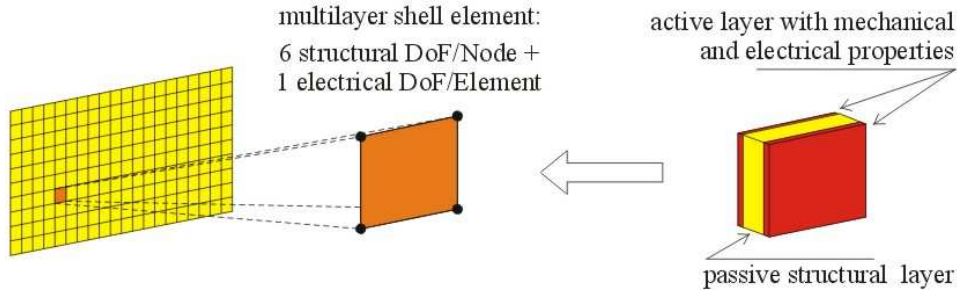


Figure 5 – FE active multilayer shell element

For this study case, the actual position of the collocated piezo-patch on the firewall is the one depicted in Fig.5. It was chosen based on previous experience, in such a way that it can sense and control most of the low-frequency modes of the firewall.

## 5 Model Reduction and State Space models

In the modeling procedure presented here, the coupled vibro-acoustic modal model is written in a state-space formulation using Matlab/Simulink. Afterwards the sensor and actuator DoFs are included in the input and output matrices respectively.

As mentioned before, due to the way fluid-structure interaction is commonly modeled in FE codes, the matrices are non-symmetric as shown in Eq.(8). Starting from the system generalized state space representation:

$$\dot{\mathbf{x}} = \begin{bmatrix} \mathbf{0} & \mathbf{I} \\ -\mathbf{M}^{-1}\mathbf{K} & -\mathbf{M}^{-1}\mathbf{C} \end{bmatrix} \mathbf{x} + [b] \mathbf{f}, \quad \mathbf{y} = [c] \mathbf{x} \quad (14)$$

where  $\mathbf{M}$ ,  $\mathbf{C}$  and  $\mathbf{K}$  are respectively the mass, damping and stiffness matrices,  $\mathbf{x}$  is the vector of states,  $\mathbf{f}$  is the load vector and  $\mathbf{y}$  is the output vector, it is possible to project it using the expression in Eq.(15). Based on the relations in Eq.(16), a reduced state-space model can be retrieved as in Eq.(17):

$$\begin{Bmatrix} \mathbf{u} \\ \mathbf{p} \end{Bmatrix} = \sum_{r=1}^{Ns+Na} q_r \begin{Bmatrix} \Phi_{Rs} \\ \Phi_{Ra} \end{Bmatrix}_r = \Phi_{R} \mathbf{q} \quad (15)$$

$$\Phi_{L}^T \mathbf{M} \Phi_{R} = \mathbf{I} \quad \text{and} \quad \Phi_{L}^T \mathbf{K} \Phi_{R} = \Omega^2 \quad (16)$$

$$\begin{Bmatrix} \dot{\mathbf{q}} \\ \ddot{\mathbf{q}} \end{Bmatrix} = \begin{bmatrix} \mathbf{0} & \mathbf{I} \\ -\Omega^2 & -\Gamma \end{bmatrix} \begin{Bmatrix} \mathbf{q} \\ \dot{\mathbf{q}} \end{Bmatrix} + \begin{bmatrix} \mathbf{0} & \mathbf{0} \\ \Phi_{Ls}^T [b_s] & \Phi_{La}^T [b_a] \end{bmatrix} \begin{Bmatrix} \mathbf{f}_s \\ \mathbf{f}_a \end{Bmatrix} \quad (17)$$

$$\begin{Bmatrix} \mathbf{u} \\ \mathbf{p} \end{Bmatrix} = \begin{bmatrix} [c_s] \Phi_{Rs} & \mathbf{0} \\ [c_a] \Phi_{Ra} & \mathbf{0} \end{bmatrix} \begin{Bmatrix} \mathbf{q} \\ \dot{\mathbf{q}} \end{Bmatrix}$$

where  $[b]$  and  $[c]$  are rectangular matrices with ones on the desired DoFs positions and zeros everywhere else, and  $\Gamma$  is the modal damping. This formulation allows the representation of the coupled vibro-acoustic system considering the mechanical influence of the piezo-patches. The modal model is built based on the diagonalized form of Eq.(8) after the modal expansion in terms of the coupled right eigenvectors furnished by Sysnoise.

In comparison with the modal expansion of Eq.(4), which requires a non-symmetric eigenproblem solution, the calculation of the modal vectors with CMS (Eq.8) are much less computationally demanding, since the modes of the uncoupled structural and uncoupled acoustic systems result from symmetric eigenvalue problems. However, the efficiency of the CMS in reducing the size of the original Eulerian model is substantially smaller if one consider the appropriate number of uncoupled acoustic modes (with

rigid boundaries) necessary to accurately represent the coupled pressure fields (with flexible boundaries). The accurate representation of the near field effects in the vicinity of the fluid-structure coupling interface requires a substantial amount of high-order modes in the acoustic modal base, which results in a higher-order modal model.

Since the objective of this paper is to validate the state-space representation of the electro-vibro-acoustic FE modal model, just a few acoustic modes were retained (Table 2), resulting in a larger reduction than it can be expected when an experimental validation is intended. In this way, the original 23552 DoFs (22697 unconstrained acoustic and 855 unconstrained structural) have been reduced to a state-space model with 54 states, 2 inputs and 2 outputs.

As shown in Eq.(12) the actuator can be represented as an extra input to the system. If one considers the modal expansion in Eq.(11) to be performed with the structural part of the coupled vibro-acoustic modal base, the first set of equations in (17) can be rewritten to include the voltage input (Eq.12). In a similar way, Eq.(13) can be included in the state-space output set of equation:

$$\begin{aligned} \begin{Bmatrix} \dot{\mathbf{q}} \\ \ddot{\mathbf{q}} \end{Bmatrix} &= \begin{bmatrix} \mathbf{0} & \mathbf{I} \\ -\boldsymbol{\Omega}^2 & -\boldsymbol{\Gamma} \end{bmatrix} \begin{Bmatrix} \mathbf{q} \\ \dot{\mathbf{q}} \end{Bmatrix} + \begin{bmatrix} \mathbf{0} & \mathbf{0} & \mathbf{0} \\ \boldsymbol{\Phi}_{\mathbf{R}s} [b_s] & \boldsymbol{\Phi}_{\mathbf{R}a} [b_a] & -\boldsymbol{\Phi}_{\mathbf{R}s}^T \mathbf{K}_{se} [b_e] \end{bmatrix} \begin{Bmatrix} \mathbf{f}_s \\ \mathbf{f}_a \\ \mathbf{V} \end{Bmatrix} \\ \begin{Bmatrix} \mathbf{u} \\ \mathbf{p} \\ \mathbf{Q} \end{Bmatrix} &= \begin{bmatrix} [c_s] \boldsymbol{\Phi}_{\mathbf{L}s} & \mathbf{0} \\ [c_a] \boldsymbol{\Phi}_{\mathbf{L}a} & \mathbf{0} \\ [c_e] \mathbf{K}_{es} \boldsymbol{\Phi}_{\mathbf{L}s} & \mathbf{0} \end{bmatrix} \begin{Bmatrix} \mathbf{q} \\ \dot{\mathbf{q}} \end{Bmatrix} \end{aligned} \quad (18)$$

Finally, the electrical-vibro-acoustic system can be represented in a first order state-space form, with force, volume velocity and voltage as inputs and displacement, pressure and charge as outputs (54 states, 3 inputs and 3 outputs.).

## 6 Results

The next sections show the results obtained using the proposed methodology. The first section deals with the system model (open-loop simulation), while the second shows some possible applications of control strategies to the coupled system.

### 6.1 Open-loop simulations

The resulting state-space model has 3 inputs and 3 outputs (Fig 6). The possible inputs are: a voltage to the piezo-patch actuator, an idealized point force at an arbitrary position on the firewall and the acoustic volume velocity source on the EC. The outputs are: the charge sensed by the piezo-patch, displacement of the force excitation point and pressure at the driver's ear position.

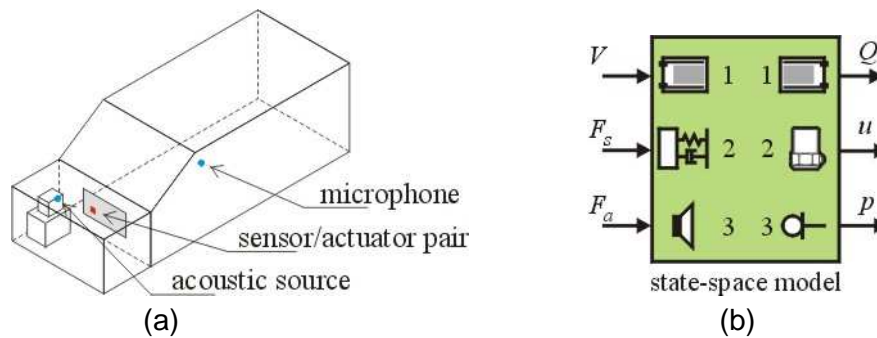
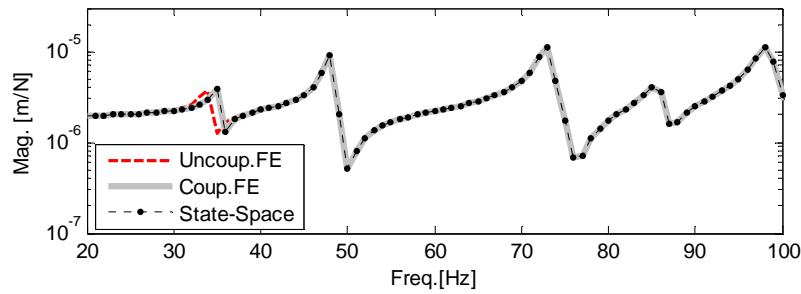


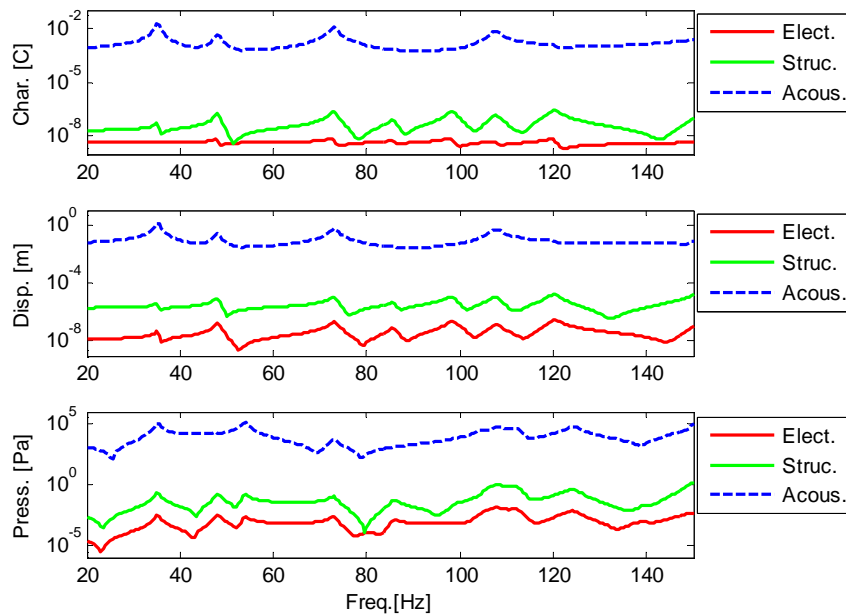
Figure 6 – Schematic view of final model (a) sensor and actuator location and (b) state space model

Figure 7 shows a comparison of structural FRFs (displacement/force) for 3 models: An uncoupled FE model of the firewall, a coupled vibro-acoustic FE model and the state-space (SS) model. As it can be seen, except for the first resonance frequency (where only the coupled FE and the SS models agree), all the models agree quite well. That is due to the weak coupling of those cavities with the 1.5mm firewall, a thinner firewall would have caused a larger coupling. However it is not possible to neglect the coupling, since an acoustic excitation is used, and therefore the structure also needs to be subject to acoustic loads.



**Figure 7 – Structural FRFs for different models**

Various combinations of output/input forced response spectra for this system are shown in Fig.8. The plots are grouped based on the output type: electric charge, displacement and pressure. The forced responses result from a unit excitation of various kinds: electric voltage, structural point force and acoustic volume velocity. It can be seen that the model is completely coupled.



**Figure 8 – Forced responses to various kinds of input**

Figure 8 illustrates also the discrepancy in the order of magnitude of the different physical quantities, *e.g.* the acoustical DoFs present much higher absolute values than the others. This particular feature is an issue when experimental system identification is concerned, as the identification algorithm could concentrate only on modeling the signals with larger amplitudes [8].

## 6.2 ASAC Simulation

As mentioned before, this modeling procedure has been developed keeping two aspects in mind: (i) the models should be suitable for control simulation and (ii) the modeling procedure should be applicable in an optimization scheme. The results presented here regard the control simulation.

An initial configuration is proposed, where a collocated SAP of piezo-patches in a velocity-feedback control loop is applied to the firewall. The basic principle of the controller is to feedback the actuator patch with an amplified voltage proportional to the time derivative of the charge generated by the sensor patch (Fig.9). The SAP position was chosen off centre (Fig.5) such that more modes could be observed and controlled by this single SAP. However, this choice was made upon previous experience rather than upon any numerical optimization method.

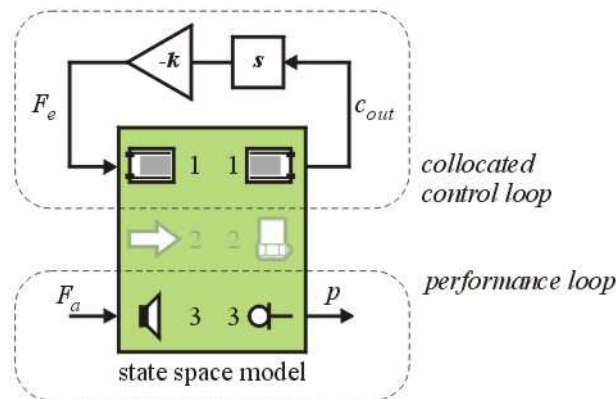


Figure 9 – Closed loop SS system

The choice of using only structural sensors and actuators is based on the robustness of the control system. When using feedback control, an important aspect to the efficiency and stability of the control system is the transfer function between the sensor and actuator. Usually, the use of acoustic sensors and/or actuators presents a fast phase decay (time delay), which would impose severe limitations to the controller frequency range [9a]. However, since the SAP is collocated (SAP transfer function with alternating poles and zeros) and based on the time derivative of the charge (which is proportional to the stress), it can be proven that the control system acts like a passive system and stability is always guaranteed [10, 11], independent of the feedback gain.

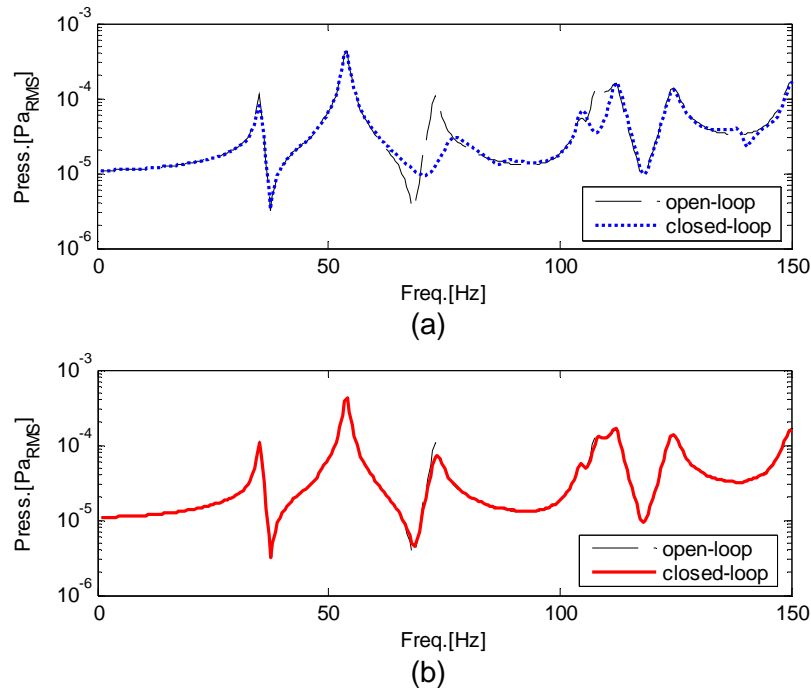
Due to the weak vibro-acoustic coupling, the structural transfer functions are much less sensitive to typical changes in this kind of systems, such as an open window or the placement of more people inside the vehicle. On the other hand, the control system only senses (directly) the structural vibration, as the acoustic resonances are barely noticeable in the structural FRFs.

Figure 10 shows the results for open and closed loop responses. The feedback gain was chosen to give the highest reduction possible within this configuration. However, as it can be seen in Fig.10a, the SAP is only efficient in damping particular modes, mainly the predominantly structural ones for which the position of the SAP offers good controllability and observability. This shows that the adequate positioning of such collocated pair is an important design parameter and therefore needs a more systematic judgment, *e.g.* by deterministic or statistical schemes [12].

Another important aspect related to those results concerns the adequate modeling of piezo-patches. The results plotted in Fig.10b are for the same SAP as in Fig.10a, however, the quasi-static behavior of the patches is taken into account by adding a high-frequency residual mode as in [13, 14]. To do so, the static structural deformation is taken for a constant voltage input on the actuator patch. The vector of structural displacements and the charge generated on the sensor patch are taken as a modal vector, which is orthonormalized with respect to the actual modal base. This residual mode is then added to the modal base as a

high-order mode (outside of the model frequency range) so that its low-frequency behavior results in a static contribution in the frequency band of interest [6, 12].

It is shown by Deraemaeker and Preumont [15], that this residual mode introduces a feedthrough component to the SAP, that if neglected, can lead to a bad estimation of the open-loop transfer function zeros and consequently to the controller performance. This error usually results in overestimating the control performance as it can be seen by comparing the results in Figs.10a and 10b, where the achievable reduction of the driver's ear sound pressure level (SPL) is respectively 0.43dB and 0.07dB.



**Figure 10 – Pressure at driver's ear for open and closed loop:  
(a) without static compensation and (b) with static compensation**

As mentioned before, an optimum feedback gain was used for both cases depicted before. Figure 11 shows how the performance (SPL at the driver's ear) varies in terms of the feedback gain. As it can be seen, both cases (with and without static compensation) present an optimum gain, related to the lowest achievable SPL. It is possible that an increase in the achievable reduction can be reached, even if the current configuration (collocated single SAP) is kept, but this solution can be accessed by an optimization routine that takes into account not only the feedback gain, but also the SAP placement. The amount of reduction could also be increased if more SAPs are placed simultaneously on the firewall. However, that measure can significantly increase the computational effort for the optimization procedure [12].

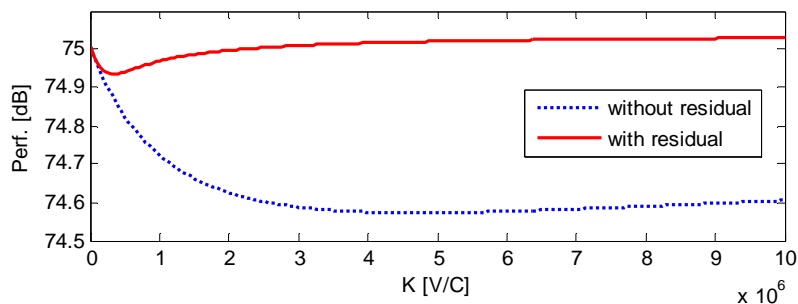


**Figure 11 – Controller performance vs. feedback gain**

## 7 Conclusions and next steps

The modeling procedure, based on reduced modal models of the vibro-acoustic system, augmented with the electrical DoFs from the piezoelectric sensor/actuator pair, succeeded in accurately representing the coupled electro-vibro-acoustic system.

The results show that the smart structure modeling approach leads to a fully coupled system where mechanical, acoustic and electrical inputs can be used as disturbance sources or control actuators. The same principle applies for the outputs, as displacement, pressure and charge can be used as monitoring or control sensors.

Special attention may be paid to the models of sensor and actuators, mainly in the case of collocated piezo-patches, where quasi-static behavior can significantly affect the sensor/actuator transfer-function zeros. This error usually results in overestimating the controller performance.

It is important to notice that the main objective of this paper was to present a methodology to simulate ASAC systems, rather than to propose a control technique for a vibro-acoustic system of this nature. In fact, besides all the advantages of a collocated controller, and the fact that such a controller would be robust against changes on the acoustic system, it presented a weak effect on damping the acoustic modes.

Concerning the placement of sensors and actuators, the use of optimization routines can be a promising approach, regarded the limitations imposed by the number of varying parameters, the complexity of the models and the computer power available. Anyway, an optimization routine should include not only the controller parameters, but also some structural features (as the thickness of a panel for example). In this way the ultimate active mechatronic system could have a better performance than that of an optimal passive structure to which a controller is added.

Although it is not the scope of this work to deal with structural optimization, Fig.12 shows how the structural design can affect the system performance. The upper part depicts the performance (in terms of total sound pressure level) of the open-loop system for various firewall thicknesses. This plot reveals that the behavior of such a system is not trivial. It is not just a matter of increasing the firewall thickness to get a lower sound transmissibility; it depends rather on the way fluid and structure interacts. The lower part of the graph shows how the uncoupled resonance frequencies of acoustic and structural components evolve with respect to the firewall thickness.

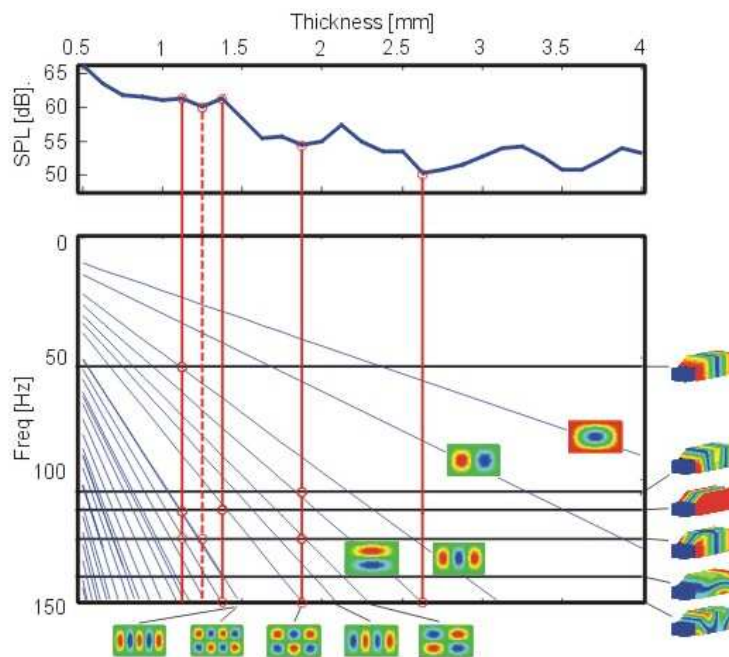


Figure 12 – Passive performance of the system with respect to the firewall thickness

It is obvious that the cavity uncoupled resonances are not affected and it is also clear that the plate resonances vary linearly with respect to the thickness. The first vertical line shows a local maximum on the performance function, related to at least 3 (well coupled) modes in the frequency band of interest. The vertical dashed line shows a local minimum, where only one acoustic mode have structural modes in its vicinities. Another interesting example comes from the line near 2mm, where apparently 3 modes have coinciding resonance frequencies but a closer look reveals that not all of them are good coupling modes (e.g. the firewall 4<sup>th</sup> mode and the cavity 2<sup>nd</sup> mode).

That will be of the same level of complexity, when an active system is to be added to such a system. Therefore an optimization routine that considers concurrently controller and structural features can definitely result in a more efficient active system.

The extension of this work regards the inclusion of other kinds of sensors and actuator models, such as accelerometers and inertia shakers. Also, the implementation of a concurrent optimization routine that takes into account, not only controller parameters (sensor/actuator position, feedback gain, etc.) but also some structural parameters (firewall thickness, geometry features, etc.) is topic of future research. The optimization routine will primarily be based on the presented smart structure modeling approach.

## Acknowledgements

Part of this research was done in the framework of the European FP 6 integrated project InMAR. This work also presents research results of the Belgian Program on Inter-University Attraction Poles initiated by the Belgian Federal Science Policy Office (AMS IAP V/06). Leopoldo de Oliveira is financed by a scholarship in the framework of a selective bilateral agreement between KU Leuven and University of São Paulo (Brazil). Arnaud Deraemaeker is currently a post-doctoral researcher of the Belgian FNRS.

## References

- [1] J.I. Mohammed, S.J. Elliott, "Active control of fully coupled structural-acoustic system" Proceeding of Inter-Noise 2005, Rio de Janeiro – Brasil (2005), 10p.
- [2] J.P. Coyette, Y. Dubois-Pèlerin, "An efficient coupling procedure for handling large size interior structural-acoustic problems" Proceedings of ISMA-19, Leuven – Belgium (1994), pp. 729-738.
- [3] N. El-Masri, M. Tournour, C. McCulloch, "Meshing procedure for vibro-acoustic models", Proceedings of ISMA 2002, Leuven – Belgium (2002), pp. 2151-2157.
- [4] W. Desmet, "A wave based prediction technique for coupled vibro-acoustic analysis", PhD Thesis, Katholieke Universiteit Leuven, Mechanical Engineering Department - PMA, 1998
- [5] Sysnoise Rev.5.3 - User's Manual - Vol.2, LMS Numerical Technologies, Leuven, Belgium
- [6] J. Luo, H.C. Gea, "Modal Sensitivity analysis of coupled acoustic-structural systems", Journal of Vibration and Acoustics, v.119 (1997), pp. 545-550
- [7] V. Piefort, "Finite Element Modelling of Piezoelectric Active Structures", PhD Thesis, Université Libre de Bruxelles, Department of Mechanical Engineering and Robotics, 2001.
- [8] W.S. Hwang, D.H. Lee, "System identification of structural acoustic system using the scale correction" Mechanical Systems and Signal Processing, 20 (2006), pp.389-402
- [9] P.A. Nelson, S.J. Elliott, *Active Control of Sound*, Academic Press, 1<sup>st</sup> Ed. (1992)
- [10] A. Preumont, *Vibration Control of Active Structures: An Introduction*, Kluwer Academic Publishers, 2<sup>nd</sup> Ed. (2002)

- 
- [11] K. Henrioulle, “Distributed actuators and sensors for active noise control”, PhD Thesis, Katholieke Universiteit Leuven, Mechanical Engineering Department – PMA, 2001
  - [12] L.P.R. Oliveira, B. Stallaert, W. Desmet, J. Swevers, P. Sas, “Optimisation Strategies for Decentralized ASAC” Proceeding of Forum Acusticum 2005, Budapest (2005), pp.875-880
  - [13] A. Deraemaeker, P. Ladevèze, Ph. Leconte., “Reduced bases for model updating in structural dynamics based on Constitutive Relation Error” *Comput. Methods Appl. Mech. Engrg.* 191 (2002) pp. 2427–2444
  - [14] E. Balmès, “Efficient sensitivity analysis based on finite element model reduction” *International Modal Analysis Conference*, Santa Barbara, (1998), pp.1-7
  - [15] A. Deraemaeker, A. Preumont, “Piezoelectric structures: modeling for control.” *Proceedings of the Ninth International Conference on Recent Advances in Structural Dynamics*, Southampton – UK, (2006), pp.11.
  - [16] L.P.R. Oliveira, M.M. Silva, G. Pinte, W. Desmet, P. Sas, P.Mas, H.Van der Auweraer, “Optimal integrated design procedure for ASAC”, *Engineering Adaptive Structures*, Maiori – Italy, (2006)

